to appear in Proceedings of
4th European Conference on Mathematics
Stockholm, 2004

Multiple Scales Asymptotics for Atmospheric Flows

Rupert Klein*, Eileen Mikusky†, Antony Owinoh†

*Mathematik & Informatik, Freie Universität Berlin
†Potsdam Institut für Klimafolgenforschung

Abstract

One important activity of theoretical meteorology involves the development of simplified model equations that describe selected scale-dependent phenomena observed in atmospheric flows. This paper summarizes a unified mathematical approach to the derivation of such models, based on multiple scales asymptotic techniques.

First we motivate the approach by an example from fluid mechanics, the interaction of small-scale quasi-incompressible flow with long-wave acoustics. In this case, the analysis proceeds via multiple scales asymptotics in terms of the Mach number, M, as the small expansion parameter. Then we discuss the particular setting of meteorology, where there is a host of singular small parameters to be taken into account. Examples are the Rossby, Froude, Mach, and Strouhal numbers. A particular distinguished limit among these parameters is introduced in combination with systematic multiple scales asymptotics. A wide range of simplified meteorological models can then be recovered by specializing this general ansatz to a single horizontal, a single vertical, and a single time coordinate.

As a concrete example we report on the multiple scales derivation of boundary layer theories. In particular, we recover the classical Ekman boundary layer equations for flows on synoptic scales ($\sim 500\,\mathrm{km}, 12\,\mathrm{h}$), and find an extension of the nonlinear Prandtl boundary layer equations to atmospheric mesoscales ($\sim 70\,\mathrm{km}, 2\,\mathrm{h}$).

1 Introduction

1.1 Single time, multiple space scales for low Mach number flows

To motivate the approach suggested here for meteorological modelling, we review the multiple scales asymptotics for low Mach number flows in [12]. Thus we discuss compressible flow with characteristic flow velocities u_{ref} that are small compared with a typical sound speed c_{ref} of the fluid, so that

$$\mathrm{M} = \frac{u_{\mathrm{ref}}}{c_{\mathrm{ref}}} \ll 1\,. \tag{1}$$

The governing Euler for compressible flow equations read

$$\begin{array}{lcll} \rho_t & + & \nabla \cdot (\rho \boldsymbol{v}) & = \ 0 \\ (\rho \boldsymbol{v})_t & + & \nabla \cdot (\rho \boldsymbol{v} \circ \boldsymbol{v}) + \dfrac{1}{\mathrm{M}^2} \, \nabla p & = \ 0 \\ (\rho e)_t & + & \nabla \cdot ([\rho e + p] \, \boldsymbol{v}) & = \ 0 \end{array} \tag{2}$$

Here $(\rho, \boldsymbol{v}, p)$ are the density, velocity, and pressure, respectively. The total energy density, ρe, obeys the equation of state,

$$\rho e = \frac{p}{\gamma - 1} + \mathrm{M}^2 \frac{\rho \boldsymbol{v}^2}{2}\,, \tag{3}$$

with γ the isentropic exponent, which is assumed constant here.

Consider a one-dimensional setting as sketched in Fig. 1. The graph on the left sketches

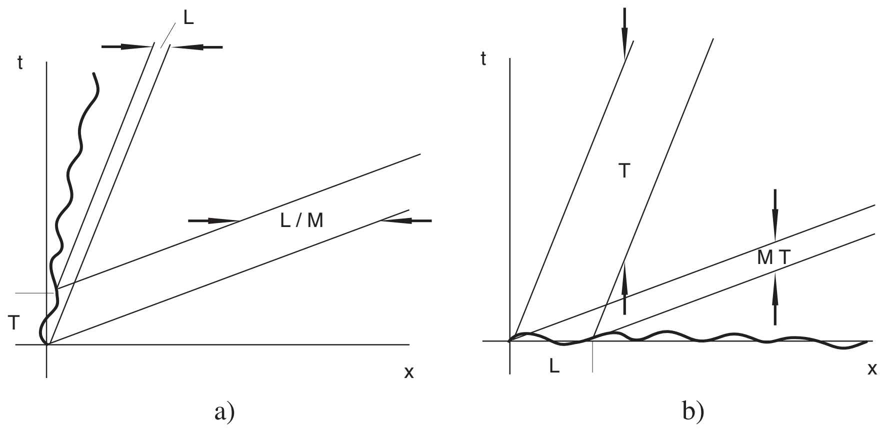

Figure 1: Single time, multiple space scales , a), vs. multiple time, single space scales, b), for low Mach number flows. Thick wiggly lines indicate perturbations, imposed locally in an oscillatory fashion, a), or with given spacial variation at some point in time, b).

a situation in which, e.g., an unstable flame drives the surrounding flow field, thereby simultaneously inducing advectively transported fluctuations of entropy, vorticity, and chemical species, and acoustic pressure perturbations. As the time scale, T, of the oscillations is imposed by the fluctuating flame, the difference in propagation speeds, $u_{\mathrm{ref}} \ll c_{\mathrm{ref}}$, results in differing characteristic lengths, L and L/M, of the associated advective and acoustic phenomena, respectively. This regime may be captured by a multiple space scale asymptotic expansion of the form, [12],

$$\mathbf{U}(\boldsymbol{x}, t; \mathrm{M}) = \sum_i \mathrm{M}^i \mathbf{U}^{(i)} \left(\boldsymbol{x}, \boldsymbol{\xi}, t\right)\,, \quad \text{where} \quad \boldsymbol{\xi} = \mathrm{M}\boldsymbol{x}\,. \tag{4}$$

The opposite regime, sketched in Fig. 1b), arises, e.g., in the solution of a Cauchy initial value Problem when the initial data have a certain characteristic length, L, and include fluctations that again excite advective as well as acoustic modes. The appropriate asymptotic representation for $\mathrm{M} \ll 1$ reads

$$\mathbf{U}(\boldsymbol{x}, t; \mathrm{M}) = \sum_i \mathrm{M}^i \mathbf{U}^{(i)}\left(\boldsymbol{x}, t, \tau\right) , \quad \text{where} \quad \tau = \frac{1}{\mathrm{M}} t \,. \tag{5}$$

In (4), (5), $\mathbf{U}$ is a placeholder for any of the dependent variables.

The second of the two regimes has been analysed in quite some detail. See, e.g., [9, 18, 5, 11, 22, 19, 10, 24, 25, 3] and the references therein. The first is less prominent, but equally important. We use it here to demonstrate how the multiple scales ansatz in (4) allows us to

1. provide a unified derivation of two well-known simplified single-scale models of theoretical fluid mechanics, and
2. derive a new extended model that explicitly describes the scale interactions in this regime.

In [12] one of the present authors derives the leading order closed set of equations that results from the expansion scheme in (4):

Pressure decomposition

$$p^{(0)} \equiv P_0(t) \,, \qquad p^{(1)} = P^{(1)}(\boldsymbol{\xi}, t) \,, \qquad p^{(2)} = p^{(2)}(\boldsymbol{x}, \boldsymbol{\xi}, t) \,. \tag{6}$$

Small scale quasi-incompressible flow

$$\begin{aligned} \rho_t \quad &+ \quad \nabla_{\boldsymbol{x}} \cdot (\rho \boldsymbol{v}) &&= \; 0 \,, \\ (\rho \boldsymbol{v})_t \quad &+ \quad \nabla_{\boldsymbol{x}} \cdot (\rho \boldsymbol{v} \circ \boldsymbol{v}) + \nabla_{\boldsymbol{x}} p^{(2)} &&= \; -\nabla_{\boldsymbol{\xi}} P^{(1)} \,, \\ & \gamma P_0 \;\; \nabla_{\boldsymbol{x}} \cdot \boldsymbol{v} &&= \; -\frac{dP_0}{dt} \,. \end{aligned} \tag{7}$$

Long wave acoustics

$$\begin{aligned} (\overline{\rho \boldsymbol{v}})_t \quad &+ \quad \nabla_{\boldsymbol{\xi}} P^{(1)} &&= \; 0 \,, \\ P_t^{(1)} \quad &+ \quad \gamma P_0 \; \nabla_{\boldsymbol{\xi}} \cdot \overline{\boldsymbol{v}} &&= \; 0 \,. \end{aligned} \tag{8}$$

Here the overbar denotes averages of the perturbation functions in the small scale variable $\boldsymbol{x}$.

Consider now the single-scale specialization of (6)–(8) for which $\nabla_{\boldsymbol{\xi}} \mathbf{U}^{(i)} \equiv 0$. In this case, $P^{(1)} \equiv P_1(t)$, and it disappears from the small scale flow equations in (7). These reduce to the well-known equations for variable density, zero Mach number flow with background compression, i.e.,

$$
\begin{aligned}
\rho_t \quad &+ \quad \nabla_{\boldsymbol{x}} \cdot (\rho \boldsymbol{v}) &&= \; 0\,, \\
(\rho \boldsymbol{v})_t \quad &+ \quad \nabla_{\boldsymbol{x}} \cdot (\rho \boldsymbol{v} \circ \boldsymbol{v}) + \nabla_{\boldsymbol{x}} p^{(2)} &&= \; 0\,, \\
&\quad\;\; \nabla_{\boldsymbol{x}} \cdot \boldsymbol{v} &&= \; -\frac{1}{\gamma P_0}\frac{dP_0}{dt}\,.
\end{aligned}
\tag{9}
$$

Consider, on the other hand, the specialization of (4) to allow only for long-wave dependencies on $\boldsymbol{\xi}$, requiring $\nabla_{\boldsymbol{x}} \mathbf{U}^{(i)} \equiv 0$. Then $dP_0/dt \equiv 0$, i.e., $P_0 \equiv P_\infty = \text{const.}$, and $\rho^{(0)} = \rho_0(\boldsymbol{\xi})$ from $(7)_3$ and $(7)_1$, respectively. The long wave equations from (8) reduce to the equations of linear acoustics with space-dependent speed of sound,

$$
\begin{aligned}
\rho_0 \boldsymbol{v}_t \quad &+ \quad \nabla_{\boldsymbol{\xi}} P^{(1)} &&= \; 0\,, \\
P_t^{(1)} \quad &+ \quad \gamma P_\infty \, \nabla_{\boldsymbol{\xi}} \cdot \boldsymbol{v} &&= \; 0\,.
\end{aligned}
\tag{10}
$$

In these equations,

$$
P_\infty = \text{const.}\,, \qquad \rho_0 = \rho_0(\boldsymbol{\xi})\,, \tag{11}
$$

and with them the sound speed $c(\boldsymbol{\xi}) = \sqrt{\gamma P_\infty / \rho_0(\boldsymbol{\xi})}$, are to be specified together with the initial data for $(P^{(1)}, \boldsymbol{v})$ to define a closed problem.

Thus, by specialization of the general multiple scales ansatz in (4) to two different single-scale versions we have recovered from (6)–(8) two well-known sets of equations from theoretical fluid mechanics.

When dependencies on both $\boldsymbol{x}$ and $\boldsymbol{\xi}$ are relevant, interactions between the small scale and long wave components of the flow will occur. One way to reveal these explicitly procedes by rewriting (6)–(8) as a system for the long wave components $\overline{\rho}, \overline{\boldsymbol{m}}, P^{(1)}, P_0$ of the flow variables and their small-scale fluctuations, $\widetilde{\rho}, \widetilde{\boldsymbol{m}}, \widetilde{p^{(2)}}$, where

$$
\boldsymbol{m} = \rho \boldsymbol{v}\,. \tag{12}
$$

First, the sublinear growth conditions on $\boldsymbol{m}$ and $\boldsymbol{v}$ for $|\boldsymbol{x}| \to \infty$ applied to $(7)_{1,3}$ allow us to conclude again that

$$
P_0 \equiv P_\infty = \text{const.}\,, \qquad \text{and} \qquad \overline{\rho^{(0)}} = \overline{\rho}_0(\boldsymbol{\xi})\,. \tag{13}
$$

These results thus do not depend on the previous assumption of a single scale dependence on $\boldsymbol{\xi}$ only, which was assumed to obtain (11). P_∞, ρ_0 are thus time independent (on the time scales considered) and are to be extracted from the initial data. The remaining unknowns $\widetilde{\rho}, \widetilde{\boldsymbol{m}}, \widetilde{p^{(2)}}$ and $\overline{\boldsymbol{m}}, P^{(1)}$ obey the

Low Mach number multiscale model:

Smallscale quasi-incompressible flow

$$\begin{aligned} \widetilde{\rho}_t &+ \nabla_{\boldsymbol{x}} \cdot (\widetilde{\boldsymbol{m}}) &= 0\,, \\ \widetilde{\boldsymbol{m}}_t &+ \nabla_{\boldsymbol{x}} \cdot (\boldsymbol{v} \circ \widetilde{\boldsymbol{m}}) + \nabla_{\boldsymbol{x}} \widetilde{p}^{(2)} &= 0\,, \\ & \nabla_{\boldsymbol{x}} \cdot \boldsymbol{v} &= 0\,, \end{aligned} \tag{14}$$

Long-wave acoustics

$$\begin{aligned} \overline{\boldsymbol{m}}_t &+ \nabla_{\boldsymbol{\xi}} P^{(1)} &= 0\,, \\ P_t^{(1)} &+ \nabla_{\boldsymbol{\xi}} \cdot \left(\overline{c}^2\, \overline{\boldsymbol{m}}\right) &= -\nabla_{\boldsymbol{\xi}} \cdot \left(\gamma P_\infty\, \overline{\widetilde{\alpha}\, \widetilde{\boldsymbol{m}}}\right)\,, \end{aligned} \tag{15}$$

where

$$\alpha = 1/\left(\overline{\rho} + \widetilde{\rho}\right)\,, \tag{16}$$

$$\boldsymbol{v} = \alpha\,\left(\overline{\boldsymbol{m}} + \widetilde{\boldsymbol{m}}\right)\,, \tag{17}$$

$$\overline{c} = \sqrt{\gamma P_\infty \overline{\alpha}}\,. \tag{18}$$

The two systems for the small scale flow and the long-wave acoustic component couple in a subtle way. The small scale flow is influenced by the long wave components $(\overline{\boldsymbol{m}}, \overline{\rho})$ through (16), (17). The two-fold influence of the small scales on the long wave modes is obvious from (15). On the left we have the operator of linear acoustics with a space-time-dependent sound speed. The latter depends on the average of the inverse density, $\overline{\alpha} = \overline{1/(\overline{\rho} + \widetilde{\rho})}$, and thus depends non-trivially on the density fluctuation $\widetilde{\rho}$. In addition, on the right of the long wave momentum equation $(15)_2$ we find a modification of the effective energy fluxes proportional to correlations of the small scale fluctuations $\widetilde{\alpha}, \widetilde{\boldsymbol{m}}$.

1.2 Organization of the paper

In analogy with the derivations of the present section we will now move to atmospheric applications. After some preliminary discussions related to the appearance of multiple small parameters in the dimensionless flow equations in section 2, we introduce a general multiple time / multiple space scale ansatz in section 3. Various specializations of this ansatz will be described which have allowed us to reproduce a host of well-known simplified model equations of theoretical meteorology. These results will be reviewed briefly in section 4. The particular example of atmospheric boundary layer flows will be discussed in more detail in section 5. Section 6 summarizes our main points and provides on outlook on ongoing and future work.

2 Dimensionless parameters and limit regimes

Atmospheric flows generally feature a very wide range of length and time scales. Simultaneously one finds turbulent fluctuations on the smallest scales, characterized by a continous spatio-temporal spectrum, and larger scale organized flow features, characterized by a relatively clean scale separation. These scale separations justify the quest for simplified model equations based on what is called *scaling analysis* in theoretical meteorology and is labelled *multiple scales asymptotics* in theoretical fluid mechanics and applied mathematics. As we will see below, such scale separations appear naturally on length and time scales comparable to or larger than about 10 km/20 min (the pressure scale height and the associated characteristic advection time scale). In the present paper we focus on simplified descriptions of scale separated phenomena, importing turbulence closures for smaller scales as "black boxes" where needed.

2.1 Dimensionless parameters for large scale atmospheric flows

There are a few physical parameters, shown in Tables 1,2, that appear to be universal to flows of the atmosphere. While the "properties of the rotating earth" deserve no further explanation, the aerothermodynamic reference values given in Table 2 should be explained.

Amongst all forces acting on the atmosphere, gravity is the strongest. As a consequence, the thermodynamic pressure is almost everywhere determined by hydrostatic balance. It follows that the pressure at some reference height, such as the mean sea level, will balance the weight of the column of air above, i.e., the sea level pressure is – to leading order – determined by the total mass of air in the atmosphere. Since gravity essentially inhibits the mass of air from leaving the planet, this reference pressure of about 1 bar may be considered a generally given constant.

The order of magnitude of the mean temperature of the atmosphere at sea level is set by the global radiative equilibrium. Even if we neglect all "green house effects" due to water vapor, CO_2, and other radiatively active species, this balance would provide for a mean temperature of about $\overline{T} \approx 250\,\mathrm{K}$. All the greenhouse effects together do substantially raise the mean temperature above this level, but not so by an order of magnitude. Through the equation of state of an ideal gas, $\rho = p/RT$, this estimate justifies the reference density given in the table.

Table 1: Properties of the rotating earth

Earth's radius	a	$\sim$	$6 \cdot 10^6$	m
rotation frequency	Ω	$\sim$	10^{-4}	s^{-1}
acceleration of gravity	g	$\sim$	10	$\mathrm{m/s^2}$

Table 2: Aerothermodynamic conditions

thermodynamic pressure	p_{ref}	$\sim$	10^5	$\mathrm{kg/ms^2}$
air flow velocity	u_{ref}	$\sim$	10	m/s
air density	ρ_{ref}	$\sim$	1	$\mathrm{kg/m^3}$

The choice of the reference flow velocity of about 10 m/s is somewhat more subtle. On the one hand, this is a characteristic value for meteorologically relevant flow velocities found almost universally in textbooks, and this may suffice to justify the present choice. There are theoretical arguments which relate this value to the mean vertical shear wind across the troposphere induced by the "thermal wind"—which is a result of the dominant momentum balances on the large scales: hydrostatics in the vertical direction, and geostrophic balance (pressure gradients balance the Coriolis force) in the horizontal direction. Figure 2 shows the long-term distribution of the zonally averaged zonal wind speed, and it corroborates the scaling in the table for most of the atmosphere.

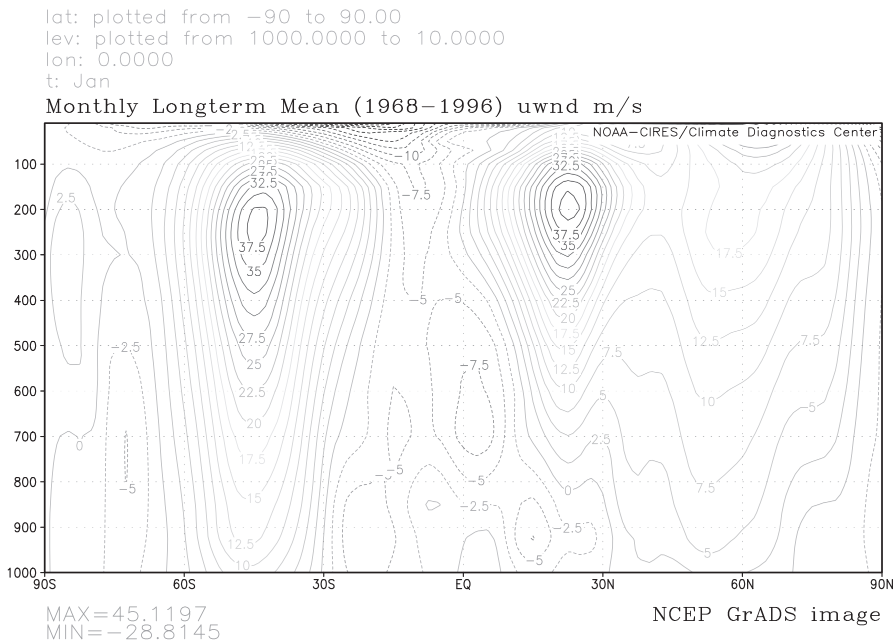

Figure 2: Magnitude of the zonal wind, in m/s, averaged zonally and over the years of 1968 to 1996. The vertical axis indicates height parameterized in terms of pressure levels and measured in mbar, the horizontal axis is the latitude in degrees. (Image provided by the NOAA-CIRES Climate Diagnostics Center, Boulder, Colorado, from their Web site at `http://www.cdc.noaa.gov/`.)

The reference values in Tables 1, 2 can be combined into three independent nondimensional characteristic numbers (six quantities involving three fundamental physical dimensions). The following combinations have proven to be useful:

$$\pi_1 = \frac{a\,\Omega}{c_{\text{ref}}} \approx 2.0\,, \qquad \pi_2 = \frac{u_{\text{ref}}}{c_{\text{ref}}} \approx 0.03\,, \qquad \pi_3 = \frac{a\,\Omega^2}{g} \approx 0.006\,. \tag{19}$$

Here $c_{\text{ref}} = \sqrt{p_{\text{ref}}/\rho_{\text{ref}}}$ characterizes the speed of sound as well as the speed of long wavelength (barotropic) gravity waves in the atmosphere.

In the attempt to construct a systematic unified approach to theoretical meteorology we seek solutions to the compressible flow equations in a rotating system that are characterized by $\pi_1 = O(1)$, whereas $\pi_2, \pi_3 \ll 1$.

Before we procede, a note on distinguished limits is in order.

2.2 Distinguished limits

Suppose we consider a differential equation in some independent variable $\boldsymbol{x}$ involving two singular small parameters, ϵ, δ, and we are interested in describing the asymptotic behavior of solutions as $\epsilon, \delta \to 0$. It is often assumed that the most general approach to this problem, at least in the single-scale setting, would be a two-parameter expansion of the solution $U(\boldsymbol{x};\epsilon,\delta)$ according to

$$U(\boldsymbol{x};\epsilon,\delta) = U^{(0)}(\boldsymbol{x}) + \epsilon U^{(1,0)}(\boldsymbol{x}) + \delta U^{(0,1)}(\boldsymbol{x}) + o(\epsilon,\delta)\,. \tag{20}$$

Such an expansion assumes the existence of the gradient (in the sense of Fréchét) of $\mathbf{U}$ with respect to ϵ, δ at $\epsilon = \delta = 0$, and of higher derivatives if higher oder terms are included.

Unfortunately, even for the simple case of the linear oscillator with small mass (say, ϵ) and small damping (say, δ), such a Fréchét derivative does not exist, because the sequential limits do not commute: If the mass vanishes first, the oscillator enters the strongly damped regime and its motion is monotonous, being governed by a balance of the spring and damping forces. If the damping vanishes first, it enters the oscillatory regime and undergoes high-frequency oscillations. Any asymptotic limit equation for the oscillator thus will depend on the path to the origin in the ϵ-δ-plane, i.e., on the particular *distinguished limit* chosen.

We conclude that distinguished limits, being a generalization of the directional or Gateau-derivative, will exist under less stringent conditions than independent two-parameter expansions. The way to proceded in the presence of the two small parameters π_2, π_3 from (19) is thus to pick some judiciously chosen distinguished limits and analyse the asymptotics of the compressible flow equations in the resulting regimes. One such limit, which is compatible with the above estimates for $\pi_1 \dots \pi_3$, has proven to be particularly useful,

$$\pi_1 \sim \varepsilon^0 = 1, \qquad \pi_2 \sim \varepsilon^2, \qquad \pi_3 \sim \varepsilon^3, \qquad \text{as} \qquad \varepsilon \to 0\,, \tag{21}$$

and this will be assumed throughout the rest of this paper.

3 Non-dimensional governing equations and general multiple scales ansatz

In nondimensionalizing the compressible flow equations with gravity and rotation below we use the reference values $(\rho_{\text{ref}}, u_{\text{ref}}, p_{\text{ref}})$ from Table 2 to measure the dependent variables, and

$$\ell_{\text{ref}} = h_{\text{sc}} = \frac{p_{\text{ref}}}{g\,\rho_{\text{ref}}} \qquad \text{and} \qquad t_{\text{ref}} = \frac{\ell_{\text{ref}}}{u_{\text{ref}}} \tag{22}$$

to measure the space and time coordinates, respectively. Here $h_{\text{sc}} \sim 10\,\text{km}$, called the pressure scale height, is the characteristic vertical distance over which the thermodynamic pressure drops appreciably in a nearly hydrostatic atmosphere.

With this understanding we consider here the governing equations

$$\begin{aligned}
\rho_t \quad &+ \quad \nabla\cdot(\rho\boldsymbol{v}) &&= \quad 0\,,\\
(\rho\boldsymbol{v})_t \quad &+ \quad \nabla\cdot(\rho\boldsymbol{v}\circ\boldsymbol{v}) + \varepsilon\,\boldsymbol{\Omega}\times\rho\boldsymbol{v} + \frac{1}{\varepsilon^4}\nabla p &&= \quad -\frac{1}{\varepsilon^4}\rho g\,\boldsymbol{k}\,,\\
(\rho e)_t \quad &+ \quad \nabla\cdot(\boldsymbol{v}\,[\rho e + p]) &&= \quad S_{\rho e}\,,
\end{aligned} \tag{23}$$

with the equation of state

$$(\rho e) = \frac{p}{\gamma - 1} + \varepsilon^4\,\frac{\rho\boldsymbol{v}^2}{2}\,, \tag{24}$$

and with $S_{\rho e}$ an effective energy source term that will not be specified further here. In practice it will include source terms from the radiative balance and from latent heat exchange due to condensation and evaporation. In (23) we have left out terms describing molecular transport or closures for turbulent transport for brevity. We will get to how the need for such closures arises naturally in a multiple scales setting in section 5.

For the reader familiar with meteorological theory we notice that the various appearances of the small parameter ε in (23) imply certain distinguished limits for the Rossby, Mach, and barotropic Froude numbers,

$$\text{Ro} = \frac{\Omega h_{\text{sc}}}{u_{\text{ref}}} \sim \frac{1}{\varepsilon}\,, \qquad \text{M} = \frac{u_{\text{ref}}}{c_{\text{ref}}} \sim \varepsilon^2\,, \qquad \text{Fr}_{\text{baro}} = \frac{u_{\text{ref}}}{\sqrt{g h_{\text{sc}}}} \sim \varepsilon^2\,. \tag{25}$$

The Rossby number being *large* may appear odd at a first glance. Yet it should be noticed that Ro as defined above is the Rossby number with respect to the pressure scale height, $h_{\text{sc}} \sim 10\,\text{km}$, not as usual with respect to the horizontal synoptic scales, $L_{\text{syn}} \sim 1000\,\text{km}$. Here we will capture flows on such large scales not by an a priori scaling of the governing equations, but by systematic use of multiple scales techniques. This will be demonstrated explicitly in the context of Ekman boundary layer theory in section 5.

4 General multiscale expansion and classical results

4.1 Multiscale expansion scheme

The equations in (23), (24), include a single small parameter ε which motivates the following asymptotic expansions. The goal is to capture the wide variety of length and time scales and associated simplified model equations of theoretical meteorology through a general multiple scales ansatz,

$$\mathbf{U}(\boldsymbol{x}, t; \varepsilon) = \sum_i \phi_\varepsilon^{(i)} \, \mathbf{U}^{(i)} \left(\dots \psi_\varepsilon^{(-1)} \boldsymbol{x}, \boldsymbol{x}, \psi_\varepsilon^{(1)} \boldsymbol{x}, \dots, \psi_\varepsilon^{(-1)} t, t, \psi_\varepsilon^{(1)} t, \dots \right) . \qquad (26)$$

Here the scaling coefficients $\psi_\varepsilon^{(j)}$ satisfy

$$\phi_\varepsilon^{(0)} = \psi_\varepsilon^{(0)} \equiv 1 \, , \qquad (27)$$

and

$$\phi_\varepsilon^{(j+1)} = o\left(\phi_\varepsilon^{(j)}\right) , \qquad \psi_\varepsilon^{(j+1)} = o\left(\psi_\varepsilon^{(j)}\right) , \qquad \text{as} \qquad \varepsilon \to 0 \, . \qquad (28)$$

The general asymptotic solution ansatz in (26) allows us to explicitly describe phenomena taking place on asymptotically separated scales, with scale ratios $\phi_\varepsilon^{(j+1)}/\phi_\varepsilon^{(j)}$ for amplitudes and $\psi_\varepsilon^{(j+1)}/\psi_\varepsilon^{(j)}$ for space and time.

The governing equations (23) involve only integer powers of ε so that an analogous choice for the scaling coefficients, i.e., $\phi_\varepsilon^{(j)} = \psi_\varepsilon^{(j)} = \varepsilon^j$ is self-suggesting. This choice allows one to derive a wide range of well-known simplified model equations of theoretical meteorology using standard asymptotics procedures. A counter-example arises in tropical meteorology, however, where non-integer powers of ε turn out to be the relevant scaling factors, see [16], and the next section.

4.2 Classical results through specializations of the general scheme

Specializing the general multiple scales ansatz from (26) by neglecting all but one time, one horizontal, and one vertical space coordinate, it could be demonstrated in [16, 13, 14] that the following simplified models of theoretical meteorology could be derived directly from the three-dimensional compressible flow equations using standard techniques of asymptotic analysis.

Coordinate scalings	Simplified model obtained
$\mathbf{U}^{(i)} = \mathbf{U}^{(i)}(t, \boldsymbol{x}, z)$	Anelastic & pseudo-incompressible models, [15, 6, 1]
$\mathbf{U}^{(i)} = \mathbf{U}^{(i)}(\varepsilon^2 t, \varepsilon^2 \boldsymbol{x}, z)$	Mid-latitude Quasi-Geostrophic model, [21, 8]
$\mathbf{U}^{(i)} = \mathbf{U}^{(i)}(\varepsilon^2 t, \varepsilon^2 \boldsymbol{x}, z)$	Equatorial Weak Temperature Gradient models, [26]
$\mathbf{U}^{(i)} = \mathbf{U}^{(i)}(\varepsilon^2 t, \varepsilon^{-1}\,\xi(\varepsilon^2 \boldsymbol{x}), z)$	Semi-geostrophic model, [21, 8, 4]
$\mathbf{U}^{(i)} = \mathbf{U}^{(i)}(\varepsilon^{\frac{5}{2}} t, \varepsilon^{\frac{5}{2}} \boldsymbol{x}, z)$	Gill's model for balanced equatorial flows, [20, 27, 7]
$\mathbf{U}^{(i)} = \mathbf{U}^{(i)}(\varepsilon^{\frac{5}{2}} t, \varepsilon^{\frac{7}{2}} x, \varepsilon^{\frac{5}{2}} y, z)$	Quasi-linear equatorial long-wave equations, [17]

Notice that all of these results have been obtained using the same distinguished limit from (21). This indicates an aspect of mutual consistency of all these models that—at least to the authors—had not been obvious to begin with.

We should mention, however, that there is one system of simplified equations, the hydrostatic primitive equations (HPEs), which is the basis of the majority of the computational weather prediction codes and climate models, and which cannot be obtained through the same distinguished limit. The only simplifying assumptions made in deriving the HPEs are that there is a dominant balance between pressure gradient and gravity in the vertical momentum equation, and that there is an (asymptotic) scale separation between the characteristic vertical and the characteristic horizontal scales. In particular, the Mach number and the barotropic Froude number based on the horizontal flow velocities are assumed to be of order $O(1)$ in this theory. In contrast, here they are small of order $O(\varepsilon^2)$ as $\varepsilon \to 0$, see (25).

The asymptotic expansion schemes shown above in the table all lead to "single scale models", because we allow for only one characteristic scale in each of the time and space directions. (The ansatz reproducing the semigeostrophic theory just allows for anisotropic horizontal scales. It is not an honest-to-goodness multiple scales expansion.)

Of course, the true potential of the general scheme in (26) may be exploited only when more than one coordinate is retained for at least one of the space-time directions. The first multiple scales application of the present approach in this sense has been presented in [16] where it was demonstrated how the approach allows one to construct systematic multiple scales models for a host of near-equatorial flow phenomena directly from the three-dimensional compressible flow equations.

In the next section we give an example of a multiple scales theory by sketching the derivations of two models describing boundary layer flows. We will also demonstrate how the necessity of "closure" or "parameterization" comes up naturally when the small-scale part of a multi-scale model enters the large scale dynamics through some nonlinear averages, yet does not allow for explicit, analytical solutions.

5 Boundary layer flows

As concrete examples of model derivations via the systematic multiple scales approach presented above we consider atmospheric boundary layer flows. In particular, we summarize the derivations for two different flow regimes which result in very different effective models.

The first ansatz reproduces the classical Ekman boundary layer theory (see, e.g., [21]). Our derivation addresses the interaction of three-dimensional flow near the ground, at characteristic spatio-temporal scales of the order of 200 m, 20 s, with middle latitude synoptic scale motions on scales of 500 km, 12 h and above. Considering that our units of measure for the space-time coordinates are $\ell_{\text{ref}} = h_{\text{sc}} \sim 10\,\text{km}$ and $u_{\text{ref}} \sim 10\,\text{m/s}$, and that $\varepsilon \sim 1/7$, the appropriate multiple scales ansatz reads

Ekman Layer Scalings:

$$\mathbf{U}(\boldsymbol{x}, t; \varepsilon) = \sum_i \varepsilon^i \, \mathbf{U}^{(i)} \left(\boldsymbol{X}, Z, T, \boldsymbol{\xi}_{\text{s}}, \tau_{\text{s}} \right) . \tag{29}$$

where

$$\boldsymbol{X} = \frac{\boldsymbol{x}_h}{\varepsilon^2} , \quad Z = \frac{z}{\varepsilon^2} , \quad T = \frac{t}{\varepsilon^2} \tag{30}$$

denote the "microscale coordinates" resolving the 200 m, 20 s scales near the ground, and

$$\boldsymbol{\xi}_{\text{s}} = \varepsilon^2 \, \boldsymbol{x}_h , \quad \tau_{\text{s}} = \varepsilon^2 \, t \tag{31}$$

are the "synoptic scale coordinates" resolving the 500 km, 12 h scales. Notice that the latter, according to the last section, are the proper horizontal and time coordinates for the derivation of quasi-geostrophic theory.

In both (30) and (31) we have anticipated that, for the scales of interest here, an approximate description of the flow in a local tangent plane to the earth surface is sufficient for our purposes. Denoting the vertical unit vector by $\boldsymbol{k}$ we have used the abbreviations

$$\boldsymbol{x}_h = (\mathbf{1} - \boldsymbol{k} \circ \boldsymbol{k}) \, \boldsymbol{x} , \qquad z = \boldsymbol{k} \cdot \boldsymbol{x} \tag{32}$$

for the local horizontal and vertical components of the position coordinate $\boldsymbol{x}$.

The second regime is relevant for the same small scales, but for 70 km, 2 h as the larger scales involved. This regime leads to a nonlinear model very similar to the classical boundary layer equations in theoretical (non-geophysical) fluid mechanics, [23], yet, it includes Coriolis effects on the larger scale. The appropriate asymptotic expansion scheme reads

Nonlinear Boundary Layer Scalings:

$$\mathbf{U}(\boldsymbol{x}, t; \varepsilon) = \sum_i \varepsilon^i \, \mathbf{U}^{(i)} \left(\boldsymbol{X}, Z, T, \boldsymbol{\xi}, \tau \right) . \tag{33}$$

where

$$\boldsymbol{\xi} = \varepsilon\, \boldsymbol{x}_h\,, \quad \tau = \varepsilon\, t\,. \tag{34}$$

5.1 Multiscale derivation of Ekman boundary layer theory

5.1.1 Leading order balances and the Boussinesq approximation

Consider the multiple scales ansatz in (29). Inserting into the governing equations (23), (24) and collecting like powers of ε we obtain a hierarchy of perturbation equations as usual. The few leading orders are dominated by the derivatives with respect to the fast variables, $\boldsymbol{X}, Z, T$. As a result we find

$$\nabla_{\boldsymbol{X}} p^{(i)} \equiv 0\,, \quad \frac{\partial p}{\partial Z}^{(i)} \equiv 0 \quad \text{for} \quad (i \in \{0,1,2,3\})\,. \tag{35}$$

We are considering here a thin boundary layer of characteristic height $O(\varepsilon^2 h_{\mathrm{sc}})$. The solution in this layer must match with the bulk flow in the atmosphere above. Thus, as usual in matched asymptotics for boundary layer flows, we find that the pressures $p^{(0)} \dots p^{(3)}$ are all imposed from outside. The natural scalings for the outer flow, compatible with the present ansatz for the boundary layer, would involve an asymptotic expansion $\mathbf{U} = \sum_i \varepsilon^i \mathbf{U}^{(i)}(\boldsymbol{\xi}_{\mathrm{s}}, z, \tau_{\mathrm{s}})$. This reproduces the well-known quasi-geostrophic theory (QG) as mentioned in the last section. In derivations not shown here, [14], we find that horizontal variations in the slow scale variables $\boldsymbol{\xi}_{\mathrm{s}}, \tau_{\mathrm{s}}$ occur first in $p^{(3)}$. As a consequence we may adopt

$$p^{(0)} \equiv P_0 = 1 = \text{const.}\,, \qquad p^{(i)} \equiv 0 \qquad (i \in \{1,2\}) \tag{36}$$

and an externally given

$$p^{(3)} \equiv P^{(3)}_{\mathrm{QG}}(\boldsymbol{\xi}_{\mathrm{s}}, \tau_{\mathrm{s}}) \tag{37}$$

from here on. It is assumed that constants for $p^{(1)}, p^{(2)}$ have been absorbed in P_0.

Order of magnitude estimates in [13, 16] for entropy fluctuations in the troposphere show that these are of order $O(\varepsilon^2)$ under typical conditions. Assuming this scaling here as well, we conclude that the "potential temperature", θ, obeys

$$\theta = \frac{p^{\frac{1}{\gamma}}}{\rho} = 1 + \varepsilon^2 \theta^{(2)} + \dots\,, \tag{38}$$

with $\theta^{(2)}(\boldsymbol{X}, Z, T, \boldsymbol{\xi}_{\mathrm{s}}, \tau_{\mathrm{s}})$ depending on the small as well as the large scale variables. For the density perturbations we conclude form (36)–(38) that

$$\rho^{(0)} \equiv \rho_0 = 1 = \text{const.}\,, \quad \rho^{(1)} \equiv 0\,, \quad \rho^{(2)} = -\theta^{(2)}\,. \tag{39}$$

The resulting leading order small scale equations are (dropping the order indicator on $\boldsymbol{u}^{(0)}, w^{(0)}$ for convenience)

$$
\begin{aligned}
(\rho_0 \boldsymbol{u})_T &+ \nabla_{\boldsymbol{X}} \cdot (\rho_0 \boldsymbol{u} \circ \boldsymbol{u}) + (\rho_0 w \boldsymbol{u})_Z + \nabla_{\boldsymbol{X}} p^{(4)} &=& \ 0\,, \\
(\rho_0 w)_T &+ \nabla_{\boldsymbol{X}} \cdot (\rho_0 \boldsymbol{u} \circ w) + (\rho_0 w^2)_Z + p^{(4)}_Z &=& \ \rho_0\, \theta^{(2)}\,, \\
(\rho_0 \theta^{(2)})_T &+ \nabla_{\boldsymbol{X}} \cdot (\rho_0 \boldsymbol{u}\, \theta^{(2)}) + (\rho_0 w\, \theta^{(2)})_Z &=& \ (\gamma - 1)\, S^{(0)}_{\rho e}\,, \\
& \nabla_{\boldsymbol{X}} \cdot \boldsymbol{v} + w_Z &=& \ 0\,.
\end{aligned}
\tag{40}
$$

These are the Boussinesq equations for small scale incompressible flow. Importantly, they include thermal effects through the buoyancy term $\rho_0 \theta^{(2)}$ in the vertical momentum balance, and through the transport equation for $\theta^{(2)}$ in the next line.

The main goal in this section is the derivation of the effective large scale boundary layer equations. The appropriate tool are sublinear growth conditions. The equations in (40) are in divergence form, so that averaging in $\boldsymbol{X}, T$ is straight forward. The resulting spatio-temporal sublinear growth conditions read

$$
\begin{aligned}
\left(\rho_0\, \overline{\overline{w^{(0)} \boldsymbol{u}^{(0)}}}\right)_Z &= 0 \\
\left(\rho_0\, \overline{\overline{w^{(0)}}}^{2} + \overline{\overline{p^{(4)}}}\right)_Z &= \rho_0\, \overline{\overline{\theta^{(2)}}} \\
\left(\rho_0\, \overline{\overline{w\, \theta^{(2)}}}\right)_Z &= (\gamma - 1)\, \overline{\overline{S^{(0)}_{\rho e}}}\,, \\
\overline{\overline{w^{(0)}}}_Z &= 0\,.
\end{aligned}
\tag{41}
$$

Here the double overbar denotes the double average in the $\boldsymbol{X}, T$ coordinates.

Taking into account the bottom boundary condition which states that the large scale average vertical velocity at $Z = 0$ vanishes (there is no vertical velocity pattern with velocity magnitude of order $O(10\,\mathrm{m/s})$ that would be coherent over distances of $O(500\,\mathrm{km})$), $(41)_4$ yields

$$
\overline{\overline{w^{(0)}}} \equiv 0\,, \tag{42}
$$

and in the sequel we define

$$
w' \equiv w^{(0)} - \overline{\overline{w^{(0)}}} = w^{(0)}\,. \tag{43}
$$

The averaging procedure $\overline{\overline{\cdot}}$ satisfies the Reynolds' averaging conditions, i.e., for some quantities $a = \overline{\overline{a}} + a'$ and $b = \overline{\overline{b}} + b'$ with $\overline{\overline{a'}} = \overline{\overline{b'}} = 0$ we have

$$
\overline{\overline{\overline{\overline{a}}\,\overline{\overline{b}}}} = \overline{\overline{a}}\,\overline{\overline{b}}\,, \qquad \overline{\overline{a'\overline{\overline{b}}}} = 0\,, \qquad \overline{\overline{a\, b}} = \overline{\overline{a}}\,\overline{\overline{b}} + \overline{\overline{a'\, b'}} \tag{44}
$$

Using (42) we conclude that

$$
\overline{\overline{w^{(0)} \boldsymbol{u}^{(0)}}} = \overline{\overline{w' \boldsymbol{u}'}}\,, \qquad \overline{\overline{w^{(0)} \theta^{(2)}}} = \overline{\overline{w' \theta'}} \qquad \overline{\overline{w^{(0)} w^{(0)}}} = \overline{\overline{w'^2}}\,. \tag{45}
$$

The same argument which we used to derive (42) may now be applied to $(41)_1$ to obtain

$$\overline{w'\,\boldsymbol{u}'} \equiv 0\,. \tag{46}$$

While, therefore, there is no large scale mean vertical transport of horizontal momentum at leading order, this is not true for the transport of vertical momentum and of heat (represented by the perturbation potential temperature, $\theta^{(2)}$). In fact, $(41)_2$ describes a modification of hydrostatics by the effective vertical momentum transport $\rho_0\overline{w'^2}$, and $(41)_3$ shows how fluctuations of vertical velocity and potential temperature must correlate to produce an effective vertical heat flux that matches the vertically integrated heat source,

$$\rho_0\,\overline{w'\theta'} = \int_0^Z (\gamma-1)\overline{S_{\rho e}^{(0)}}\,dZ\,. \tag{47}$$

For later reference we notice that, in analogy with $(41)_3$, the first and second order potential temperature equations also represent a balance of fluxes and source terms, so that

$$\left(\overline{\rho w\theta}^{(i)}\right)_Z = (\gamma-1)\;S_{\rho e}^{(i-2)} \qquad \text{for} \qquad i\in\{1,2\}\,. \tag{48}$$

5.1.2 Three-term balance in the Ekman layer

We are interested here in exhibiting the relation of the present multiple scales derivations with Ekman boundary layer theory. This theory addresses the balance of horizontal momentum on large space and time scales. In the present setting we consider, in analogy with $(41)_1$, the sublinear growth conditions from the horizontal momentum equations at first, second, and third order. These are (we add the earlier result for completeness)

$$\begin{aligned}
\partial_Z\,(\overline{\rho w\boldsymbol{u}})^{(0)} &= 0\,,\\
\partial_Z\,(\overline{\rho w\boldsymbol{u}})^{(1)} &= 0\,,\\
\partial_Z\,(\overline{\rho w\boldsymbol{u}})^{(2)} &= 0\,,\\
f\boldsymbol{k}\times\rho_0\overline{\boldsymbol{u}^{(0)}} + \nabla_{\boldsymbol{\xi}}P_{\rm QG}^{(3)} + \partial_Z\,(\overline{\rho w\boldsymbol{u}})^{(3)} &= 0\,.
\end{aligned} \tag{49}$$

Here $f=\boldsymbol{k}\cdot\boldsymbol{\Omega}$ is the vertical component of the earth rotation vector in the considered tangent plane. Thus we recover the Ekman boundary layer theory's three-term balance equation for horizontal momentum in $(49)_4$.

A few remarks are in order here:

(i) Flow evolution on the length and time scales assumed in Ekman theory requires very weak correlations of the flucutations of density and the vertical and horizontal

velocities. Because of the no-slip bottom boundary condition, equations $(49)_1$–$(49)_3$ imply

$$(\overline{\rho w \boldsymbol{u}})^{(i)} \equiv 0 \qquad \text{for} \qquad i \in \{0, 1, 2\}\,.$$

(ii) The three-term balance in $(49)_4$ is obtained here allowing general entropy (potential temperature) perturbations of order $O(\varepsilon^2)$. As seen in the Boussinesq equations governing the small scale, (40), as well as in the equation describing the large scale vertical thermal flux, (47), such perturbations are sufficient to induce leading order small scale vertical motions. Thus the present derivations are valid for thermally driven as well as for thermally neutral flows.

(iii) Depending on whether such thermal fluctuations are present or not, the structure of the small scale flow will differ considerably, and so will the relation between the effective Ekman layer momentum flux $\overline{\rho w \boldsymbol{u}}^{(3)}$ and the large scale mean flow.

(iv) Classical Ekman theory, [21], assumes thermally neutral flow and uses a simple gradient flux approximation to represent the vertical momentum flux. That is, in $(49)_4$ we would have

$$(\overline{\rho w \boldsymbol{u}})^{(3)} = -\rho_0\, K_m \frac{\partial \overline{\boldsymbol{u}^{(0)}}}{\partial Z}$$

and the Ekman layer equation becomes (dropping $^{(0)}$ for the moment)

$$\frac{\partial^2}{\partial Z^2}\,(\overline{\boldsymbol{u}} - \boldsymbol{u}_{\rm QG}) + \frac{f}{K_m}\boldsymbol{k} \times (\overline{\boldsymbol{u}} - \boldsymbol{u}_{\rm QG}) = 0\,.$$

This is the classical Ekman layer equation for the deviation $(\overline{\boldsymbol{u}} - \boldsymbol{u}_{\rm QG})$ of the horizontal mean flow velocity from the quasi-geostrophic large scale flow that prevails above the boundary layer. Solutions must satisfy the boundary and asymptotic matching conditions

$$(\overline{\boldsymbol{u}} - \boldsymbol{u}_{\rm QG}) = -\boldsymbol{u}_{\rm QG} \quad \text{at} \quad (Z = 0)\,,$$

and

$$(\overline{\boldsymbol{u}} - \boldsymbol{u}_{\rm QG}) \to 0 \quad \text{as} \quad (Z \to \infty)\,.$$

There are exact solutions to this problem which exhibit a spiral vertical distribution of the horizontal large scale flow velocity throughout the layer: As we leave the layer, vertical derivatives vanish asymptotically and we approach geostrophic balance of Coriolis force and pressure gradient. As a consequence, flow velocity and pressure gradient are orthogonal to each other—the flow velocity is tangent to level set of the pressure field.

In contrast, near the ground the flow velocity and the Coriolis force vanish, and we have a balance of pressure gradient and the effective vertical momentum transport term. The vertical shear, and with it the velocity close to the ground, thus have to be aligned with the pressure gradient.

(v) The present derivations are somewhat incomplete, at least for the case of thermally driven layers. In the presence of second order density perturbations another somewhat thicker boundary layer will establish within which the mean vertical fluxes are dominated entirely by buoyant updrafts. A detailed analysis of this regime is beyond the scope of this paper.

5.2 Boundary layer with advective nonlinearity

Here we consider the modified boundary layer scalings from (33). All the leading perturbation equations up to the first appearance of derivatives with respect to the large scale variables $\boldsymbol{\xi}, \tau$ are unchanged in this regime, and so are the associated sublinear growth conditions. Thus, all the results from (35) to $(49)_3$ remain valid.

We are interested here in the modification of the large scale evolution equations in the presence of mesoscale variations. The sublinear growth conditions from the third order horizontal momentum and potential temperature equations read

$$\overline{\theta^{(2)}}_{\tau} + \nabla_{\boldsymbol{\xi}} \cdot \left(\overline{\boldsymbol{u}^{(0)} \theta^{(2)}} \right) + \frac{1}{\rho_0} \left(\overline{\rho w \theta} \right)_Z^{(5)} = (\gamma - 1) \overline{S_{\rho e}^{(3)}} \,, \tag{50}$$

$$\overline{\boldsymbol{u}^{(0)}}_{\tau} + \nabla_{\boldsymbol{\xi}} \cdot \left(\overline{\boldsymbol{u}^{(0)} \circ \boldsymbol{u}^{(0)}} \right) + f \boldsymbol{k} \times \left(\overline{\boldsymbol{u}^{(0)}} - \boldsymbol{u}_{\mathrm{QG}} \right) + \frac{1}{\rho_0} \left(\nabla_{\boldsymbol{\xi}} \overline{p^{(4)}} + (\overline{\rho w \boldsymbol{u}})_Z^{(3)} \right) = 0 \,, \tag{51}$$

In addition to their counterparts in the Ekman-regime, $(49)_4$ and $(41)_3$, these euqations involve the local time derivative, and horizontal advection in the form of a nonlinearly averaged effective transport term. The latter cannot be expressed in terms of the large scale variables only without further approximation. However, under the reasonable assumption that the leading, first, and second order correlations involving the horizontal velocity components vanish in analogy with the decorrelation observed for the horizontal and vertical velocities in $(49)_1$–$(49)_3$, we may simplify these terms. In this case, e.g.,

$$\overline{\boldsymbol{u}^{(0)} \circ \boldsymbol{u}^{(0)}} = \overline{\boldsymbol{u}^{(0)}} \circ \overline{\boldsymbol{u}^{(0)}} \,, \qquad \overline{\boldsymbol{u}^{(0)} \theta^{(2)}} = \overline{\boldsymbol{u}^{(0)}} \; \overline{\theta^{(2)}} \,. \tag{52}$$

There is one more difference between the present mesoscale regime and the Ekman regime considered in the last subsection. As the horizontal scale considered here is by one order of magnitude smaller than in the former regime, the horizontal large scale flow divergence is by one order of magnitude larger here. In fact, a detailed analysis of the first order mass continuity equations shows that

$$\nabla_{\boldsymbol{\xi}} \cdot \overline{\boldsymbol{u}^{(0)}} + \partial_Z \overline{w^{(3)}} = 0 \,, \tag{53}$$

whereas the analogue of this equation in the Ekman regime would have involved $w^{(4)}$. Therefore, there will generally be a coherent large scale vertical velocity at third order, i.e., $\overline{w^{(3)}} \neq 0$. Taking into account that the vertical flux terms, $(\overline{\rho w \boldsymbol{u}})^{(3)}$, $\left(\overline{\rho w \theta}\right)^{(3)}$ will thus have a coherent contribution from large scale vertical advection by $\overline{w^{(3)}}$ we may rewrite as

$$
\begin{aligned}
\left(\overline{\rho w \boldsymbol{u}}\right)^{(3)} &= \overline{w^{(3)}}\;\overline{\boldsymbol{u}^{(0)}} + \left(\overline{\rho w' \boldsymbol{u}'}\right)^{(3)} \\
\left(\overline{\rho w \theta}\right)^{(5)} &= \overline{w^{(3)}}\;\overline{\theta^{(2)}} + \left(\overline{\rho w' \theta'}\right)^{(5)} .
\end{aligned}
\tag{54}
$$

This decomposes the flux terms into large scale coherent advection and net fluxes resulting from nonlinear averages over small scale fluctuations.

We summarize the boundary layer equations for this regime in a streamlined notation using the following replacements,

$$
\overline{\boldsymbol{u}^{(0)}} \to \boldsymbol{u}\,, \qquad \overline{w^{(3)}} \to w\,, \qquad \overline{p^{(4)}} \to p\,, \qquad \overline{\theta^{(2)}} \to \theta\,. \tag{55}
$$

Nonlinear Boundary Layer Equations:

$$
\begin{aligned}
\frac{D\boldsymbol{u}}{D\tau} + f\boldsymbol{k} \times (\boldsymbol{u} - \boldsymbol{u}_{\mathrm{QG}}) + \frac{1}{\rho_0}\nabla_{\boldsymbol{\xi}} p &= -\frac{1}{\rho_0}\left(\overline{\rho w' \boldsymbol{u}'}\right)^{(3)}_Z , \\
\frac{D\theta}{D\tau} &= -\frac{1}{\rho_0}\left(\overline{\rho w' \theta'}\right)^{(5)}_Z + (\gamma - 1)\overline{S^{(3)}_{\rho e}} , \\
\frac{1}{\rho_0} p_Z - \theta &= -\left(\overline{{w^{(0)}}^2}\right)_Z , \\
\nabla_{\boldsymbol{\xi}} \cdot \boldsymbol{u} + w_Z &= 0 .
\end{aligned}
\tag{56}
$$

Here $\boldsymbol{u}_{\mathrm{QG}}$ is the flow velocity outside the boundary layer, and

$$
\frac{D}{D\tau} = \partial_\tau + \boldsymbol{u} \cdot \nabla_{\boldsymbol{\xi}} + w\,\partial_Z . \tag{57}
$$

These equations resemble the classical Prandtl boundary layer equations in that, in addition to the vertical fluxes from nonlinear small-scale averages, they explicitly include the unsteady term and advection both in the horizontal and vertical directions. In addition, however, they include Coriolis effects and internal gravity waves, the latter arising due to the interaction of potential temperature transport in $(56)_2$ with the horizontal momentum balance in $(56)_1$ via the hydrostatic balance in $(56)_3$.

6 Closing Remarks

This paper has summarized a unified approach to meteorological modelling. It uses judiciously chosen distinguished limits among the multiple singular parameters of the system, and systematic multiple scales asymptotics based on the remaining $\varepsilon \ll 1$. We have outlined how a wide range of well-established simplified “single scale” models of theoretical meteorology can be recovered naturally through this approach. Here "single scale" means that only a single characteristic scale is assumed for any of the coordinate directions and for time, respectively.

Two aspects of these re-derivations of established theories seem worth noting:

- The small expansion parameter, ε, is a representative of a particular distinguished limit amongst the various singular small parameters of the system, i.e., of the Rossby, Froude, Mach, and other characteristic numbers. One and the same distinguished limit turns out to be adequate for the derivation of most of the simplified models considered.
- All derivations use the full three-dimensional compressible flow equations as the starting point.

The approach naturally lends itself as a tool to study multiple scales interactions. A first successful application was the derivation of "Systematic multi-scale models for the tropics" in [16], which led to very promising further developments, [2]. Here we have discussed a recent analysis of atmospheric boundary layer flows as an example of a typical multi-scale application.

First we have revisited the flow regime of the classical Ekman boundary layer theory involving $\sim 500\,\mathrm{km}, 12\,\mathrm{h}$ length and time scales, respectively. We were able to reproduce Ekman's theory which describes the quasi-stationary balance of the Coriolis, pressure gradient and (turbulent) friction terms. We obtained these classical results by replacing the nonlinear averages of vertical advective fluxes, which naturally arise in sublinear growth conditions from the multiple scales technique, with certain simplified closures normally imported from turbulence theory. However, our derivations also demonstrate how such closures may be improved once additional information on the small scale flow becomes available.

We have then considered flows on the "meso scales" covering $\sim 70\,\mathrm{km}, 2\,\mathrm{h}$. Here we found a very different set of boundary layer equations describing inherently unsteady effects, advection both in the horizontal and in the vertical direction, and nonlinear inertio-gravity waves. The latter are wave motions being driven simultaneously by Coriolis effects and by the mechanisms for internal gravity waves.

Acknowledgments

The authors thank Ann S. Almgren, Julian C.R. Hunt, Andrew J. Majda, and V. Petukhov for fruitful discussions and encouragement, and the *Deutsche Forschungsgemeinschaft* for their continuing support under grants KL 611/6, KL 611/14.

References

[1] Bannon P.R., 1995: Potential vorticity conservation, hydrostatic adjustment, and the anelastic approximation, *J. Atmos. Sci.*, **52**, 2302–2312

[2] Biello J.A., Majda A.J., 2004: A new multi-scale model for the Madden-Julian oscillation, submitted to *J. Atmos. Sci.*

[3] Cheverry C., 1996: The modulation equations of nonlinear geometric optics, *Comm. Part. Diff. Eqs.*, **21**, 1119–1140

[4] Cullen M.J.P., 2000: On the accuracy of the semi-geostrophic equations, *J. Roy. Met. Soc.*, **126**, 1099–1116

[5] DiPerna R., Majda A.J., 1985: The validity of nonlinear geometric optics for weak solutions of conservation laws, *Comm. Math. Phys.*, **98**, 313–347

[6] Durran D. R., 1989: Improving the anelastic approximation, *J. Atmos. Sci.*, **46**, 1453–1461

[7] Gill A.E., 1980: Some simple solutions for heat-induced tropical circulation, *Quart. J. Roy. Meteor. Soc.*, **106**, 447–462

[8] Gill A.E., 1982: Atmosphere-Ocean Dynamics, Academic Press

[9] Hunter J., Keller J., 1983: Weakly nonlinear high frequency waves, *Comm. Pure & Appl. Math.*, **36**, 547–569

[10] Joly J.L., Métivier G., Rauch J., 1993: Resonant one-dimensional nonlinear geometric optics, *J. Funct. Analysis*, **114**, 106–231

[11] Klein R., Peters N., 1988: Cumulative effects of weak pressure waves during the induction period of a thermal explosion in a closed cylinder, *J. Fluid Mech.*, **187**, 197–230

[12] Klein R., 1995: Semi-implicit extension of a Godunov-type scheme based on low Mach number asymptotics I: One-dimensional flow, *J. Comp. Phys.*, **121**, 213–237

[13] Klein R., 2003: An applied mathematical view of theoretical meteorology, invited presentation, in: Proc. ICIAM 2003, Sydney, Australia

[14] Klein R., Mikusky E., Vater S., 2004: Mathematische Modellierung in der Klimaforschung (in german), Lecture Notes, FB Mathematik & Informatik, Freie Universität Berlin

[15] Lipps F., Hemler R.S., 1982: A scale analysis of deep moist convection and some related numerical calculations, *J. Atmos. Sci.*, **39**, 2192–2210

[16] Majda A.J., Klein R., 2003: Systematic multi-scale models for the tropics, *J. Atmos. Sci.*, **60**, 393–408

[17] Majda, A., 2003: Introduction to PDE's and waves for the atmosphere and ocean, American Mathematical Society

[18] Majda A.J., Rosales R.R., 1984: Resonantly interacting weakly nonlinear hyperbolic waves: I. A single space variable, *Stud. Appl. Math.*, **71**, 149–179

[19] Majda A.J., Rosales R.R., Schönbek M., 1988: A canonical system of integrodifferential equations arising in resonant nonlinear acoustics, *Stud. Appl. Math.*, **79**, 205–262

[20] Matsuno, T., 1966: Quasi-geostrophic motions in the equatorial area, *J. Meteor. Soc. Japan*, Ser II, **44**, 25–43

[21] Pedlosky J., 1987: Geophysical Fluid Dynamics, Springer Verlag

[22] Pego R., 1988: Some explicit resonating waves in weakly nonlinear gas dynamics, *Stud. Appl. Math.*, **79**, 263–270

[23] Schlichting H., Gersten K., 2003: Boundary-Layer Theory, 8th edition, Springer Verlag

[24] Schochet S., 1994: Resonant nonlinear geometric optics for weak solutions of conservation laws, *J. Diff. Eqs.*, **113**, 473–504

[25] Schochet S., 1994: Fast singular limits of hyperbolic PDEs, *J. Diff. Eqs.*, **114**, 476–512

[26] Sobel A., Nilsson J., Polvani L., 2001: The weak temperature gradient approximation and balanced tropical moisture waves. *J. Atmos. Sci.*, **58**, 3650–3665

[27] Webster P.J., 1972: Response of the tropical atmosphere to local steady forcing, *Mon. Wea. Rev.*, **100**, 518–541